Supplementary Information

Facile fabrication of hollow carbon nanomaterials by directed polymerization of butadiyne on the surface of reverse micelles

Sara Jahani, Jean-François Morin, Anna M. Ritcey**

Département de chimie and Centre de Recherche sur les Matériaux Avancés (CERMA)

1045 Ave de la Médecine, Université Laval, Québec, Canada G1V 0A6

1. Butadiyne monomer synthesis

The detailed synthesis protocol of the butadiyne monomer and ^{1}H NMR data have been reported in our previous publication.[S1]

2. Critical packing parameter

Table S1 illustrates how variations in the surfactant molecular geometry defined by the critical packing parameter (Ps) lead to different structures, including normal spherical, cylindrical, inverse spherical micelles, and lamellar.

Table S1. Surfactant assembled morphologies as a function of Ps

Ps	Surfactant	Micelle	Micelle name
Ps < 1/3	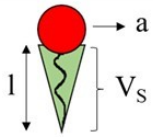		Normal Spherical micelle
1/3 < Ps < 1/2		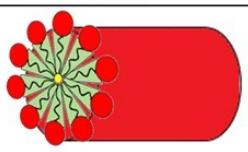	Normal cylindrical micelle
Ps ~ 1	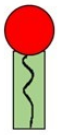	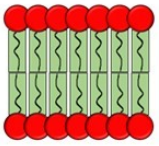	Lamellar phase
Ps > 1	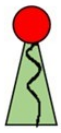	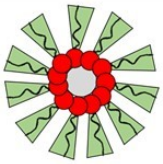	Inverse spherical micelle

3. Particle size determination

According to the transmission electron microscopy (TEM) images, the carbon nanospheres have an average diameter of 5.4 nm (Figure S1). The carbon nanorods have an average diameter of 3.1 nm (Figure S2). There are the hollow spheres and hollow rods with average size of 3.3 nm and 2.3 nm in sample d (Figure S3).

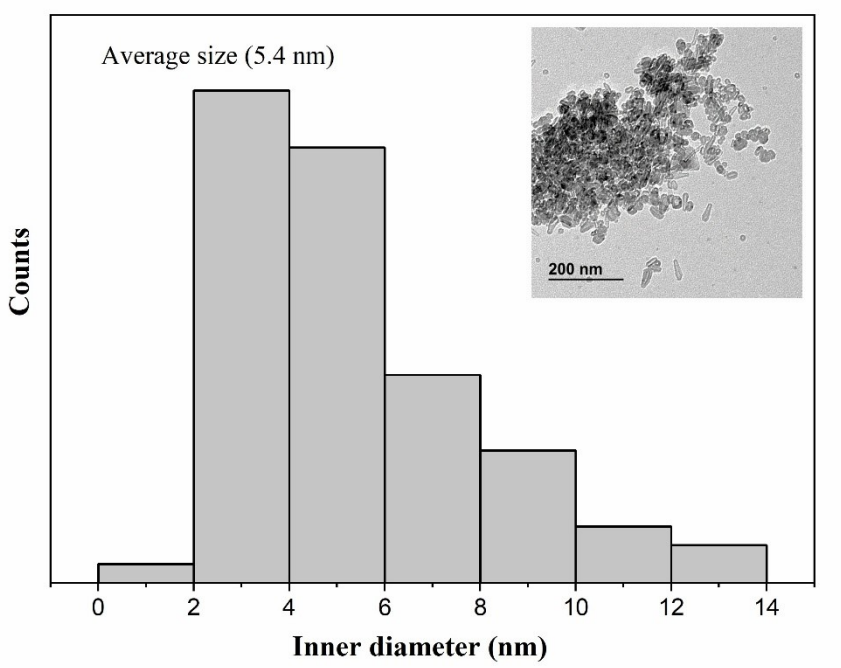

Figure S1. Size distribution histogram of sample (a) obtained from TEM image.

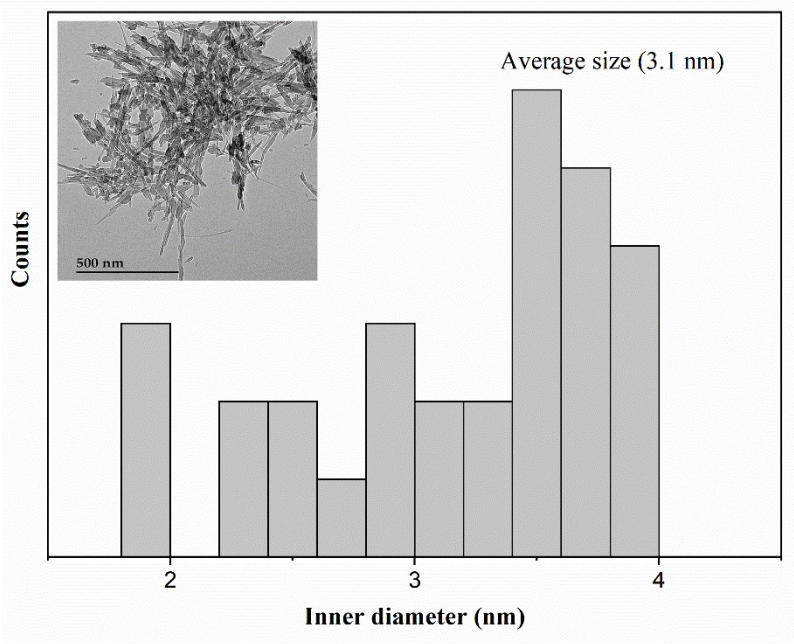

Figure S2. Size distribution histogram of sample (b) obtained from TEM image.

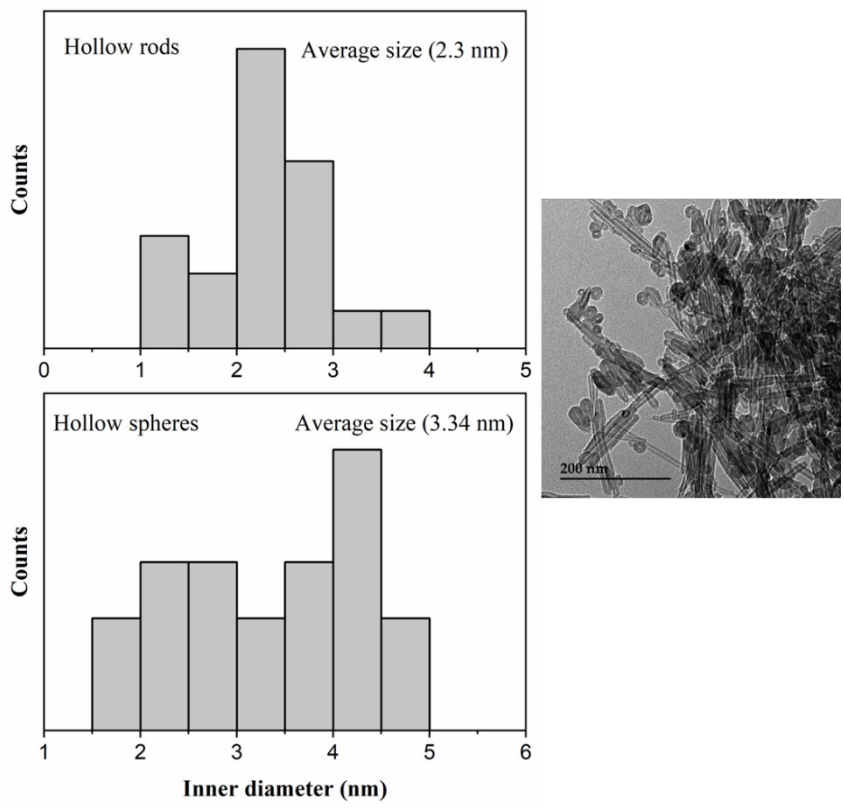

Figure S3. Size distribution histogram of sample (d) obtained from TEM image.

4. Dynamic Light Scattering (DLS)

The results show that increasing the water content slightly shifts the micelle size distribution toward larger diameters. However, the overall size range remains narrow. As shown in Figure S4, an increase in the water content from 2 to 5 results in an increase in micelle size on the order of 2 nm. The range of spherical micelle sizes achievable by varying the water content is too narrow to significantly affect the size of the resulting hollow carbon nanospheres.

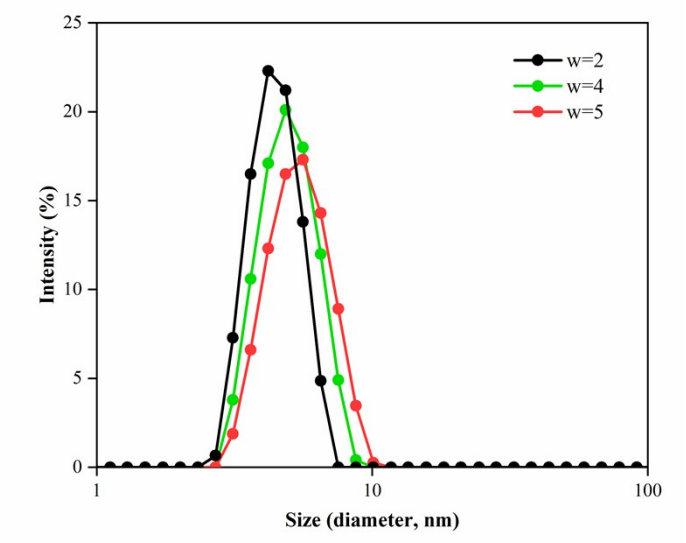

Figure S4. DLS analysis of micelle size distributions at different water contents (w = 2, 4, and 5).

5. Energy-dispersive X-ray spectroscopy (EDS)

The chemical composition of the samples was analyzed by EDS. The results indicate that carbon is the predominant element in all synthesized nanomaterials. The EDS spectra obtained for all the samples are very similar and the spectrum of sample **c** is shown in Figure S5 as an example. In addition to carbon, signals are observed from gold and palladium, used in the coating process, as well as from silicon and oxygen present in the silicon wafer substrate.

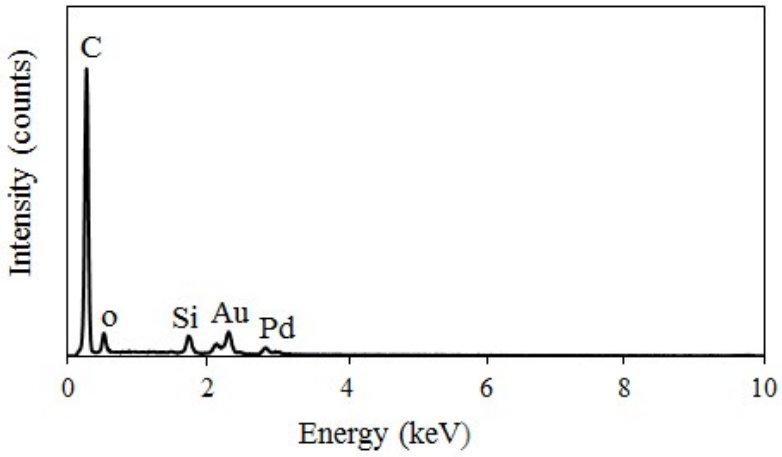

Figure S5: EDS analysis of sample **c**.

6. X-ray photoelectron spectroscopy (XPS)

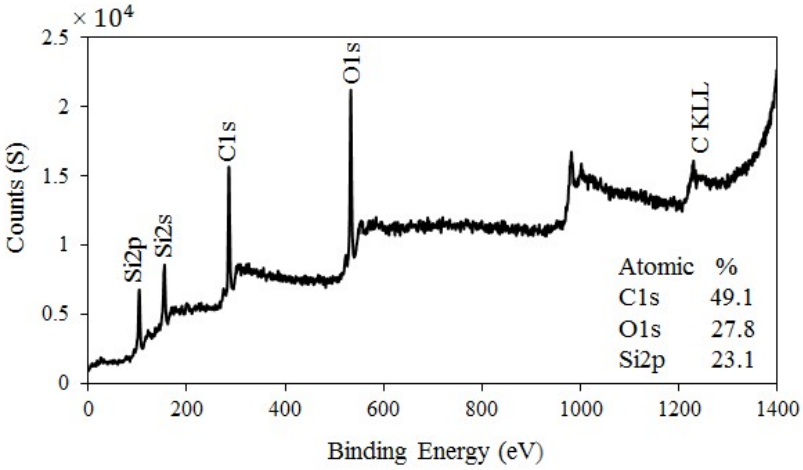

Figure S6. XPS survey spectrum for sample **c**.

7. Reproducibility of the synthesis

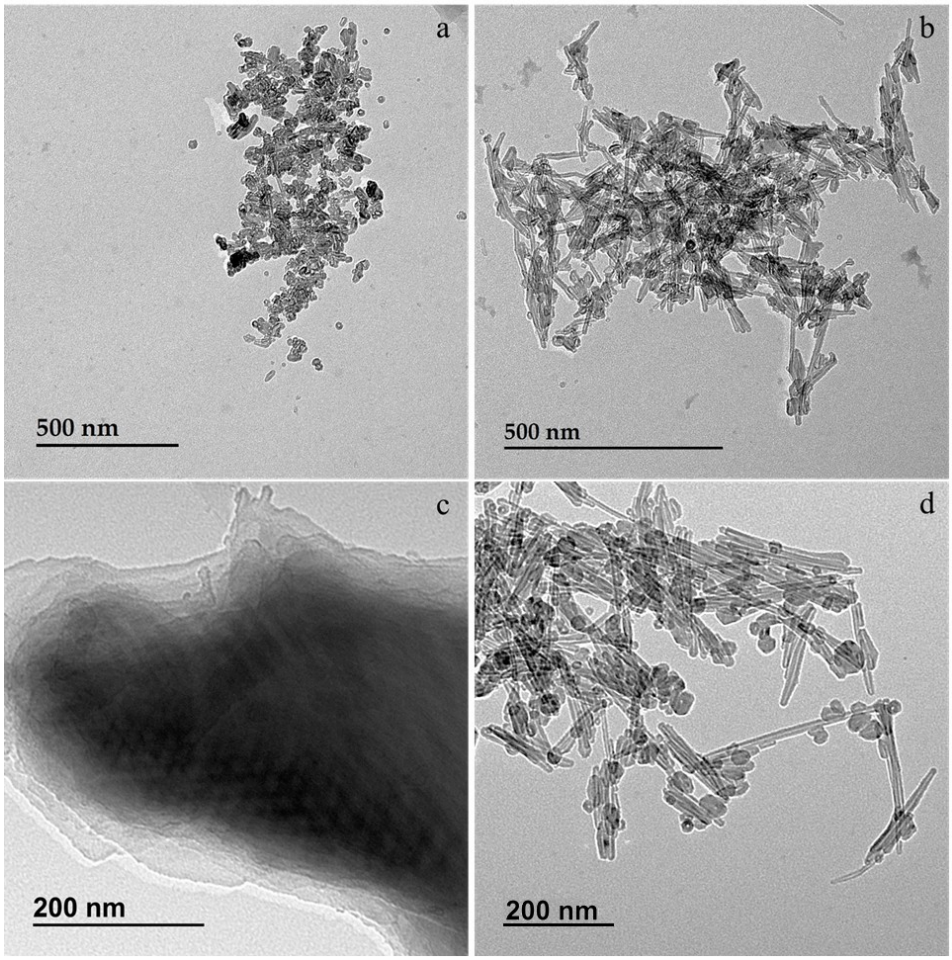

Figure S7. TEM images of carbon nanomaterials in different morphologies: hollow carbon nanospheres (a), carbon nanorods (b), carbon honeycomb-like layers (c), and a mixture of hollow carbon nanorods and nanospheres (d), synthesized using copper (II) fluoride as the copper source. While the observed morphologies are similar to those in Figure 1, this figure highlights the same morphological outcomes obtained using a different copper source.

References

(S1) Jahani, S.; Morin, J. F.; Ritcey, A. M. Twisted Graphene Synthesis via Lamellar Template Polymerization for Optoelectronic Applications. *ACS Appl. Nano Mater.* **2025**, *8* (37), 17952–17958. https://doi.org/10.1021/acsanm.5c02965.